

We are IntechOpen, the world's leading publisher of Open Access books Built by scientists, for scientists

4,800

Open access books available

122,000

International authors and editors

135M

Downloads

Our authors are among the

154

Countries delivered to

TOP 1%

most cited scientists

12.2%

Contributors from top 500 universities



WEB OF SCIENCE™

Selection of our books indexed in the Book Citation Index
in Web of Science™ Core Collection (BKCI)

Interested in publishing with us?
Contact book.department@intechopen.com

Numbers displayed above are based on latest data collected.
For more information visit www.intechopen.com



Highly accurate geometric correction for NOAA AVHRR data

An Ngoc Van
Institute of Industrial Science, University of Tokyo
Japan

Mitsuru Nakazawa and Yoshimitsu Aoki
Graduate School of Science and Technology, Keio University
Japan

1. Introduction

Since 1970, AVHRR (Advanced Very High Resolution Radiometer) on board the NOAA (National Oceanic and Atmospheric Administration) series of satellites has been an ideal observatory for daily global observation of the Earth. NOAA AVHRR data provides very useful information about ecosystems, climate, weather and water from all over the world. It is also widely used for land cover monitoring at global and continental scales.

NOAA AVHRR data are presented in the image coordinate system. Frequently, however, information extracted from AVHRR data is integrated with map data or given to consumers in a map-like form. Therefore, it is necessary to transform NOAA AVHRR data from the image coordinate system into the map coordinate system. In those applications using NOAA AVHRR data, geometric correction with high accuracy plays a very important role to ensure that NOAA AVHRR data is precisely transformed from one coordinate system to another.

Some geometric correction methods for NOAA AVHRR data, or NOAA images, have been proposed. The most popular methods can be divided into two types: orbital geometry model and transformation based on ground control points (GCPs). In the former, the knowledge about the characteristics of the satellite is used to build a physical model that defines the sources of error and the direction as well as the magnitude of their effects. However, this type of method is based on only nominal parameters. It takes into account only selected factors that cause geometric distortion. Variations in the altitude or attitude of the satellite are not considered because the information needed to correct caused by these variations is not generally available (Mather, 2004). The latter looks at the problem from the opposite of view. Rather than attempt to construct the physical model that produces errors, it uses an empirical method to compare the differences between the positions of GCPs, which can be identified both on the image and on the map of the same area. From the differences between the distributions of GCPs on the image and on the map, the errors can be estimated and removed (Mather, 2004). Recently, precise geometric correction method (Ono & Takagi, 2001; Takagi, 2003), which uses GCP template matching and considers elevation effect, has obtained accurate results by considering residual errors and elevation effect when acquiring the errors,

as well as applying affine transform to correct them. Although the precision of this method is high, the errors still exist on the rough regions after correction.

In order to improve the precision of the geometric correction for NOAA AVHRR data, this book chapter is dedicated to introduce a novel highly accurate geometric correction method. Section 2 of this chapter will write about NOAA AVHRR data, the steps of NOAA AVHRR data processing (including geometric correction) and the applications relating to NOAA AVHRR data. Section 3 will review the current geometric correction methods, which used orbital geometry model or GCP model, to point out the advantages and disadvantages of each type of those methods. Based on the analysis in section 3, section 4 will introduce a novel highly accurate geometric correction for NOAA AVHRR data, which takes the advantage of the method using GCP and adds more input data to make the result more accurate. This section will also give some discussions on the novel method. The final section will be conclusion and future works.

2. NOAA AVHRR data

2.1 NOAA POES satellites

Eight years from establishment, in October 1978, NOAA launched TIROS-N, their first POES satellite. This series of satellites continued with the satellites from NOAA-6 to NOAA-14, which were launched from 1979 to 1994. In the spring of 1998, a new series of NOAA POES satellites commenced with the launch of NOAA-K. NOAA-K and its immediate successors, such as NOAA-L and NOAA-M, NOAA-N, represented an improvement over the previous series of satellites. Figure 1 is a NOAA POES satellite (NASA, 2002).



Fig. 1. A NOAA POES satellite

POES satellite's orbit is near-polar orbit, which means the satellite travels from the pole to pole, and the angle between the equatorial plane and the satellite orbital plane is nearly 90 degrees. With the altitude between 830km and 870km, NOAA POES satellites can cover the most difficult-to-cover parts of the world. NOAA POES satellites operate in a sun-synchronous orbit, so they pass the equator and each latitude at the same local solar time each day. This feature enables regular data collection at consistent times as well as long-term comparisons (NOAA, 1998)(NOAA, 2000). NOAA has two polar-orbiting meteorological satellites in orbit

at all times (NOAASIS-a, 2008). Together they provide twice-daily global coverage, and ensure that data for any region of the earth are no more than 6 hours old. The swath width, the width of the area on the Earth's surface that the satellite can "see", is approximately 2,500km (NOAA, 1998)(NOAA, 2000).

2.2 AVHRR sensor

NOAA POES satellites use Advanced Very High Resolution Radiometer (AVHRR) as the instrument to collect data from the Earth. AVHRR uses passive detection. Each sensor on board an AVHRR instrument is corresponding to a channel, which is designed to record information from a different range of wavelengths, from visible to infrared. The first AVHRR was a 4-channel radiometer, first carried on TIROS-N (launched October 1978). This was subsequently improved to a 5-channel instrument (AVHRR/2) that was initially carried on NOAA-7 (launched June 1981). The latest instrument version is AVHRR/3, with channel 3 is divided into 3A and 3B, first carried on NOAA-K launched in May 1998. The sensors scan line by line as the satellite moves forward along its track. This forward motion of the satellite is used to build up an image by the collection of the scan lines.

2.3 NOAA AVHRR data

After the information of Earth's surface is recorded by the sensors, it is sent from the satellite to the ground receiving stations in a raw digital format. This data is NOAA AVHRR data and is stored in a digital image (NOAA AVHRR image or NOAA image) including the recorded data lines. Figure 2 is the channel 4 of a NOAA image received in Tokyo, Japan in August 1998.

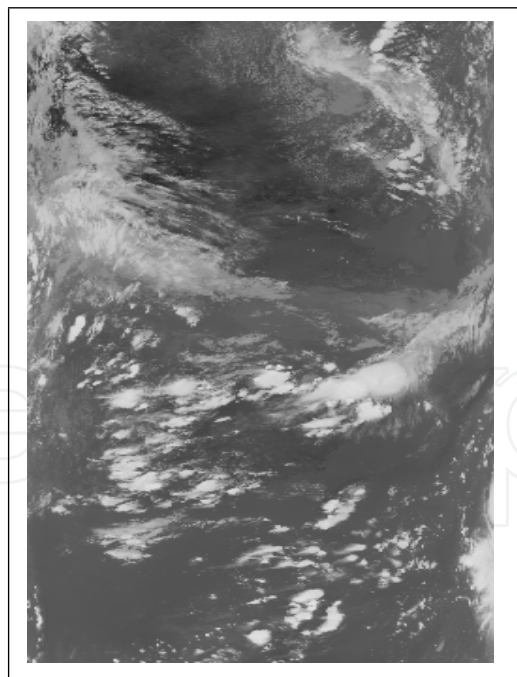


Fig. 2. Channel 4 of a NOAA image received in Tokyo, Japan in August, 1998

A NOAA image contains the lines scanned by the AVHRR sensors. Each line includes the data from all 5 channels of the AVHRR sensors. Every channel in a line contains 2048 pixels. The value of a pixel is coded in 10 bits. The highest spatial resolution of NOAA AVHRR image is

1.1km, which means that one pixel at the nadir of the satellite is corresponding with an area of 1.1km by 1.1km. The resolution of the pixels at the edges of the images is lower (Mather, 2004).

2.4 Data processing

Many image processing and analysis techniques have been applied to extract as much information as possible from the NOAA images. These techniques often include three basic steps: preprocessing, image enhancement, and information extraction. The data processing begins with the correction of the errors by some degree of preprocessing including one or more of cosmetic correction, geometric correction, atmospheric correction and radiometric correction. After preprocessing step, image enhancement operations are carried out to improve the interpretability of the image by increasing apparent contrast among various features in the scene. Information Extraction is the last step toward the final output of the remote sensing data processing.

Both image enhancement and information extraction steps are deployed on the output of preprocessing step. Therefore, the accuracy in the data preprocessing, including geometric correction, plays a very important role in the precision of remote sensing data processing.

2.5 The applications of NOAA AVHRR data

Because of the polar orbiting nature of the POES series satellites, these satellites are able to collect global data on a daily basis for a variety of land, ocean, and atmospheric applications. NOAA AVHRR data supports a broad range of environmental monitoring applications including weather analysis and forecasting, climate research and prediction, global sea surface temperature measurements, atmospheric soundings of temperature and humidity, ocean dynamics research, volcanic eruption monitoring, forest fire detection, global vegetation analysis, search and rescue, and many other applications. Nowadays, NOAA AVHRR data is also combined with high-resolution remote sensing data such as MODIS, LANDSAT TM, SPOT HRVÉ to extract very useful information.

3. Review on geometric correction for NOAA AVHRR data

3.1 Geometric distortions

NOAA AVHRR data, as other types of remote sensing data, obtained by the satellite often contains geometric distortions. These distortions can be caused by the Earth's rotation, the velocity variations in the scanning process and forward movement of the satellite during the acquisition of data, the variations of Earth's elevation and the orbit height. Geometric distortions are generally divided into two types: systematic distortion and non-systematic distortion (Gibson & Power, 2000).

Systematic distortions are introduced by the remote sensing system itself or in combination with Earth's rotation or curvature characteristics. These distortions include: skew, variation in ground resolution, and displacement or scale distortion. Most systematic distortions can be corrected using the data obtained from accurate monitoring of the satellite's orbital path and the knowledge of the scanning system's characteristics.

Non-systematic distortions are usually introduced by phenomena that vary in nature through space and time. These distortions result mainly from variations in the satellite's orbit and terrain's features, which usually involve altitude and attitude changes. Geometric non-systematic distortions can be corrected only by using ground control points (Murai, 1980). A ground control point (GCP) is a location on the surface of the Earth (e.g., a road intersection, a river intersection) that can be identified easily on the image and located accurately on

a map. The image analyst must be able to obtain two distinct sets of coordinates associated with each GCP, which are image coordinates (e.g., specified in i rows and j columns) and map coordinates (e.g., x, y measured in degrees of latitude and longitude). The paired coordinates (i, j and x, y) from many GCPs can be modeled to derive geometric transformation coefficients to correct the distortions (Mather, 2004).

Figure 3a is an example of the skew distortion caused by the Earth rotation effect. The dotted rectangle is the image received from satellite; the solid parallelogram is the data after correction. Due to the Earth's eastwards rotation, the start of each scan line is displayed slightly westwards. Figure 3b is an example of the distortion caused by altitude change. The dotted rectangle is the image received from satellite; the solid trapezium is the data after correction. Due to the altitude change, a trapezium on the Earth's surface becomes a square in the remote sensing image.

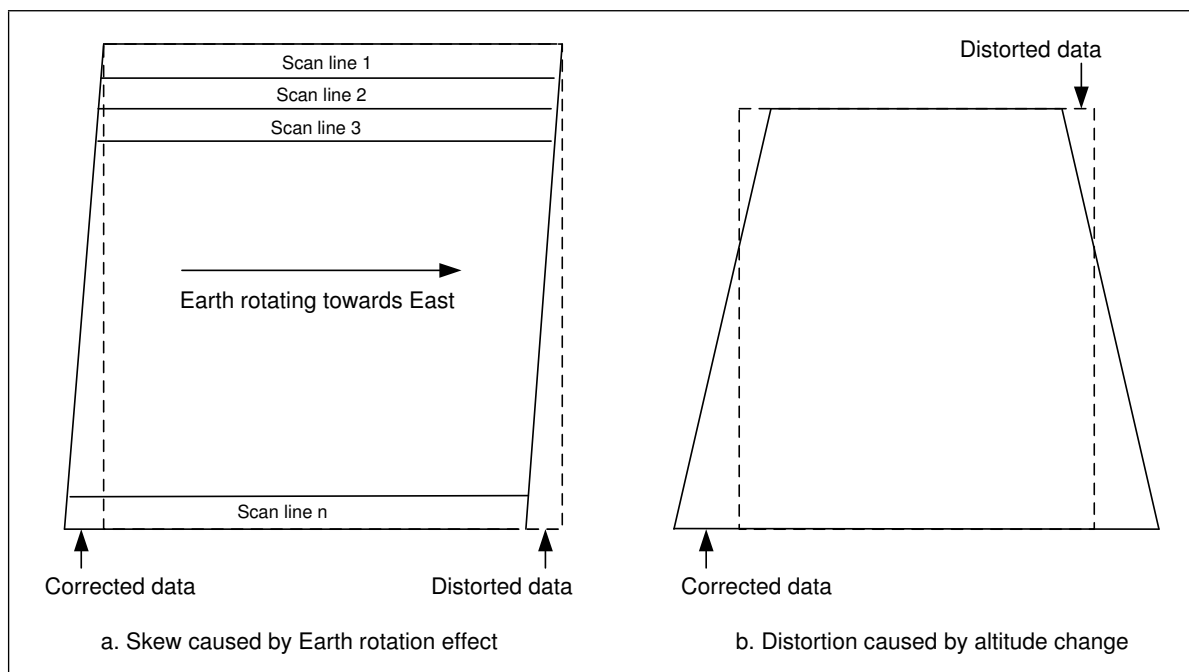


Fig. 3. Geometric distortions

3.2 Geometric corection

Geometric correction process can be considered to include these operations: (1) determination of a relationship between the coordinate system of map and image or image and image, (2) establishment of a set of points defining pixel centers in the corrected image that, when considered as a rectangular grid, define an image with the desired cartographic properties, and (3) estimation of pixel values to be associated with those points (Mather, 2004).

Based on these operations, a lot of geometric correction methods have been proposed. Generally, geometric correction methods can be divided into two types: the methods based on the nominal parameters and the methods based on the map (Mather, 2004).

In the former, the knowledge about the characteristics of the satellite's orbit is used to build a physical model that defines the sources of error and the direction as well as the magnitude of their effects. For example, Bannari (Bannari et al., 1995) used the properties of the satellite orbit and the viewing geometry to relate the image coordinate system to the geographical

coordinate system. Another method that corrects the coordinate system of remote sensing images using approximate orbit parameters was proposed by Landgrebe (Landgrebe, 1980). In this method, the orbital parameters are used to express and correct the distortions, such as the skew caused by Earth rotation effect. This type of methods is based upon only the nominal parameters than the actual orbital parameters. Only the selected factors that cause geometric distortions are taken into account. The variations in the altitude or attitude of the satellite are not considered because the information needed to correct for these variations is not generally available.

The latter looks at the problem from the opposite of view. Rather than attempt to construct the physical model that defines the sources of errors and the direction and magnitude of their effects, an empirical method is used which compares the differences between the positions of the GCPs on the image and on the map. From the differences between the distribution of GCPs on the image and the distribution of GCPs on the map, the nature distortions present in the image can be estimated, and an empirical transformation to relate the image and map coordinate systems can be computed and applied. This empirical function should be calibrated (using GCPs), applied to the image, and then validated (using separate test set of GCPs) (Mather, 2004). The correction methods based on map is used to correct the non-systematic distortions, which are caused by attitude and altitude change.

For NOAA AVHRR data, both types of geometric correction methods are described (Brush, 1985; Crawford et al., 1996; Moreno & Melia, 1993; Purevdorj & Yokoyama, 2000; Saitoh et al., 1995; Tozawa, 1983). However, most of them did not consider or considered insufficiently the non-systematic distortions produced by the altitude change, particularly the terrain relief. As mentioned by Mather (Mather, 2004), the altitude change can cause very considerable distortions in the satellite images. If this type of distortion can be corrected, the results of geometric correction will be improved significantly. Therefore, the method to correct this type of distortion in NOAA images is important.

Recently, precise geometric correction method (Ono & Takagi, 2001; Takagi, 2003; Yasukawa et al., 2004), which is based on GCPs and considers the elevation effect, has obtained accurate results. In this method, the variation effect is considered to acquire the distortion more precisely. The next section will explain the precise geometric correction method in more detail.

3.3 Precise geometric correction for NOAA AVHRR data

In the precise geometric correction method (Ono & Takagi, 2001; Takagi, 2003), because the error correction in the image coordinate system is more accurate than the one in the map coordinate system, the errors in NOAA images are corrected in the image coordinate system before the images are transformed into the map coordinate system. Figure 4 shows the steps of this method.

3.4 GCP Template Matching considering elevation effect

3.4.1 Elevation effect

Elevation effect is caused by elevation error. Figure 5 is an example of the schematic illustration of the situation that the elevation error occurs (O is the center of Earth, $R_e = 6378.14\text{km}$ is the Radius of Earth, $r = 7228\text{km}$ is the distance OC). There is a mountain at A , the top of this mountain is D whose height is h . The data the satellite receives from D should be assigned to A with the scanning angle θ_1 . However, because the satellite does not take the height h into account, the data it receives from D is assigned to A' with scanning angle θ_2 . In this case, AA' is elevation error.

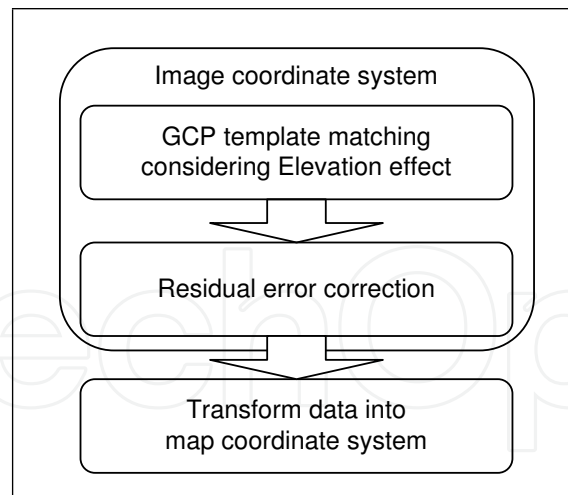


Fig. 4. Steps of the Precise Geometric Correction Method

In the rectangle ODC, DC is found based on θ_1 , Re , r and h ; and the relationship between θ_2 and the sides is represented by (1). Because $OC = r$ and $OD = Re + h$, θ_2 is found as (2).

$$OD^2 = DC^2 + OC^2 - 2.DC.OC.\cos\theta_2 \quad (1)$$

$$\theta_2 = \cos^{-1} [(DC^2 + r^2 - (Re + h)^2) / (2.r.DC)] \quad (2)$$

As point out in (Takagi, 2003), the difference of the scan angles ($\theta_2 - \theta_1$) is directly proportional to the elevation error; furthermore, because OC (7228km) is much bigger than BC (satellite's height: 830km), the angles ϕ_1 and ϕ_2 in the figure 2 are very small. Therefore, AA' can be calculated as (3) (unit: pixel) (Takagi, 2003), where 1024 (pixels) is the half width of a NOAA images, and maximum scan angle of AVHRR sensor is 55.4° .

$$AA' = (\theta_2 - \theta_1) * 1024 / 55.4 \quad (3)$$

The elevation errors are dominant in longitude direction near equator and in latitude direction near polar region in the map coordinate system, which corresponds to the pixel direction in the image coordinate system. The higher the area is, the bigger its elevation error is. The elevation data is read from GTOPO30 dataset, whose resolution is 0.008 degree in both latitude and longitude directions. This elevation data can be used to correct the elevation errors in NOAA images because the resolution of AVHRR mapping system is 0.01 degree.

3.4.2 GCP Template Matching

In the precise geometric correction method, it is very important to accurately acquire the residual errors, which present the displacement of a point from incorrect to correct position. Residual errors are measured by GCP template matching. The information about GCP templates is stored in the Digital Chart of the World. GCP templates are selected from the coastlines (such as the coastline of islands) and the inland objects (such as the coastline of lakes or rivers), which have robust features to specify the displacement (Takagi, 2003).

GCP template matching starts with the generating of GCP templates in the map coordinate system. The size of each template is 33x33 pixels. These templates are then transformed into the image coordinate system. In order to correct the elevation errors for GCP templates, each point in every template is moved in the pixel direction according to its elevation error.

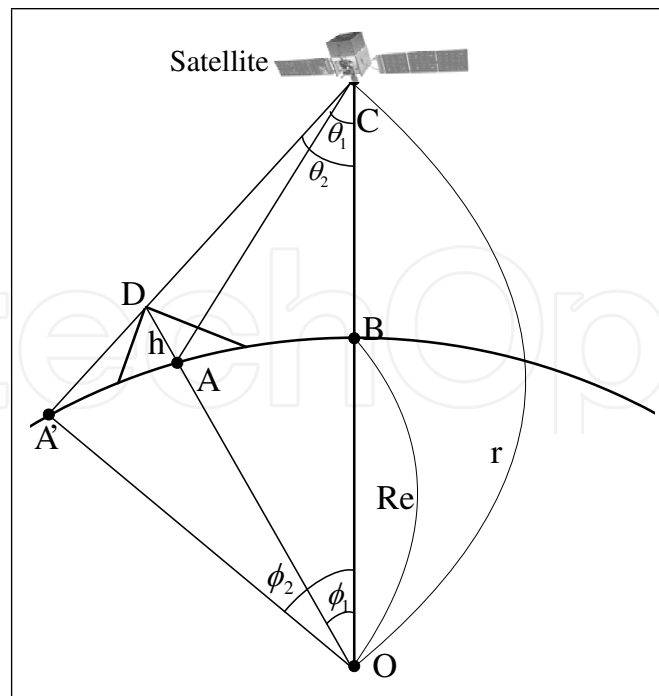


Fig. 5. Schematic illustration of the situation that elevation error occurs

Next, the pieces of 65x65 pixels of the original image corresponding to GCP templates are selected. They are binarized to create the binary and edge images. After binarizing, the piece 65x65 pixels and the GCP template are matched by SSDA (Takagi, 2003) to find out the best matching position.

3.5 Residual Error Correction

In order to specify the residual errors, the positions of the coastlines in the image coordinate system are generated from the coastline data in the map coordinate system considering the elevation effect. The coastlines are then compared with the GCP templates, whose positions are already matched by GCP template matching. The displacements from the positions of GCP templates to the coastlines are residual error vectors, which are used to present residual errors. Finally, the affine transform are used to correct the residual error vectors (Ono & Takagi, 2001; Takagi, 2003).

Affine transform is used to calculate the error $(\Delta l, \Delta p)$ for each point (l, p) in the image coordinate system. The error $(\Delta l, \Delta p)$ is calculated as follow:

$$\begin{pmatrix} \Delta l \\ \Delta p \end{pmatrix} = \begin{pmatrix} \alpha_{11} & \alpha_{12} \\ \alpha_{21} & \alpha_{22} \end{pmatrix} \begin{pmatrix} l \\ p \end{pmatrix} + \begin{pmatrix} \beta_1 \\ \beta_2 \end{pmatrix} \quad (4)$$

where α_{11} , α_{12} , α_{21} , α_{22} , β_1 and β_2 are the coefficients which are specified based on residual error vectors by the precise geometric correction method (Ono & Takagi, 2001).

The correct position of the point (l, p) will be calculated by (5):

$$\begin{cases} l & = & l + \Delta l \\ p & = & p + \Delta p \end{cases} \quad (5)$$

According to the correction process, because affine transform is applied to calculate error vectors, the variation of elevation is considered as a linear variation on all regions. However,

in fact, the variation of elevation on rough regions is complicated; therefore, affine transform will produce incorrect results, especially on the rough regions.

3.6 Transforming Data into the Map Coordinate System

In the final step, NOAA data in the image coordinate system is transformed into the map coordinate system. In order to transform, the data in the map coordinate system is divided into the blocks of 16x16 points and the position in the image coordinate system of each block is calculated. Figure 6 is an example of this transformation. Figure 5a is a block of 16x16

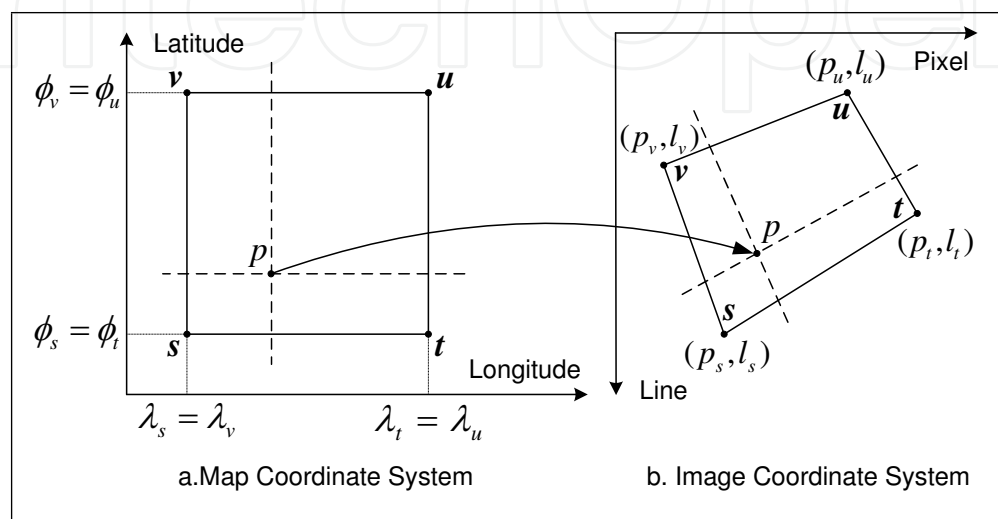


Fig. 6. Bilinear Interpolation

points in the map coordinate system; the position in the image coordinate system of this block is shown in the figure 5b. Firstly, the positions in the image coordinate system of four corner points s , t , u and v in this block are precisely calculated based on the parameters of the satellite and earth's location. Next, the position in the image coordinate system of the point p inside this block is interpolated from four corner points by using bilinear interpolation with (6) (Ono & Takagi, 2001), where E_s , E_t , E_u , E_v are the elevation errors of s , t , u , v , correspondingly. This process is repeated for all blocks. Finally, the data in the image are assigned to the correct positions in the map.

$$\left\{ \begin{array}{l} l_p = \left(\begin{array}{l} (\phi_v - \phi_p)(\lambda_t - \lambda_p)l_s \\ + (\phi_p - \phi_s)(\lambda_t - \lambda_p)l_v \\ + (\phi_v - \phi_p)(\lambda_p - \lambda_s)l_t \\ + (\phi_p - \phi_s)(\lambda_p - \lambda_s)l_u \end{array} \right) / (\phi_v - \phi_s)(\lambda_t - \lambda_s) \\ p_p = \left(\begin{array}{l} (\phi_v - \phi_p)(\lambda_t - \lambda_p)(p_s + E_s) \\ + (\phi_p - \phi_s)(\lambda_t - \lambda_p)(p_v + E_v) \\ + (\phi_v - \phi_p)(\lambda_p - \lambda_s)(p_t + E_t) \\ + (\phi_p - \phi_s)(\lambda_p - \lambda_s)(p_u + E_u) \end{array} \right) / (\phi_v - \phi_s)(\lambda_t - \lambda_s) \end{array} \right. \quad (6)$$

Referred to (6), the elevation errors of the points inside a block are interpolated from the elevation errors of only four corner points. For this reason, (6) will produce correct result on

only the flat blocks; it will be incorrect on the rough blocks, where the variation of elevation is complicated.

4. Highly accurate geometric correction for NOAA AVHRR data

By considering elevation effect, the precise geometric correction method (Ono & Takagi, 2001)(Takagi, 2003) has improved the correction result. After correction, the residual errors are considerably reduced. However, as shown in the previous chapter, the precise geometric correction method still has some problems:

- Because affine transform is applied to calculate the residual errors, the variation of elevation error is considered as a linear variation on all regions of the image. However, the variation of elevation error is complicated, especially on the rough regions, it cannot be considered as a linear variation on all regions. Therefore, affine transform will produce incorrect residual error correction result.
- By using bilinear interpolation to transform data from the image coordinate system into the map coordinate system, the elevation errors of the points inside a block are interpolated from the elevation errors of the corner points of that block. For this reason, bilinear interpolation will have correct result only on the flat blocks, where the difference of the elevation errors between the corner points and the rest points inside the block is small; it will be wrong on the rough blocks, where the variation of elevation is big.

In order to increase the precision of geometric correction for NOAA AVHRR data, this section proposes a new geometric correction method. The proposed method solves the problems of the precise method by considering the variation of elevation. Depending on the variation of elevation, residual errors are corrected by different transforms on different regions; data is also transformed into the map coordinate system by different methods on different regions. Additionally, to make GCP template matching to be more precise, more GCP templates are automatically generated from the feature of the coastline.

4.1 Steps of the proposed method

Figure 7 shows the steps of the proposed method.

4.2 Finding flat and rough blocks

As mentioned above, when using affine transform to calculate the residual errors, the results on the rough regions are not good because the variation of elevation is complicated on these regions and affine transform is not able to express it; therefore, affine transform should be applied only on the flat regions, where the difference of elevation between to neighboring points is small. On the other hand, when transforming data from the image coordinate system into the map coordinate system by using bilinear interpolation, because the elevation error of a point inside a block is interpolated from the elevation errors of four corner points, bilinear interpolation will produce errors on rough regions. For these reasons, to identify flat and rough regions is necessary to reduce the error.

In order to find out the flat and rough block, the data in the map coordinate system is divided into blocks of 16x16 points. The elevation data of every point in each block are read from GTOPO30 dataset. The highest and lowest points in each block are compared to decide if it is flat or rough block. If a block is rough, it will be divided into four same-size smaller blocks. The dividing process is repeated on the rough blocks until the sizes of all rough blocks are 4x4 points.

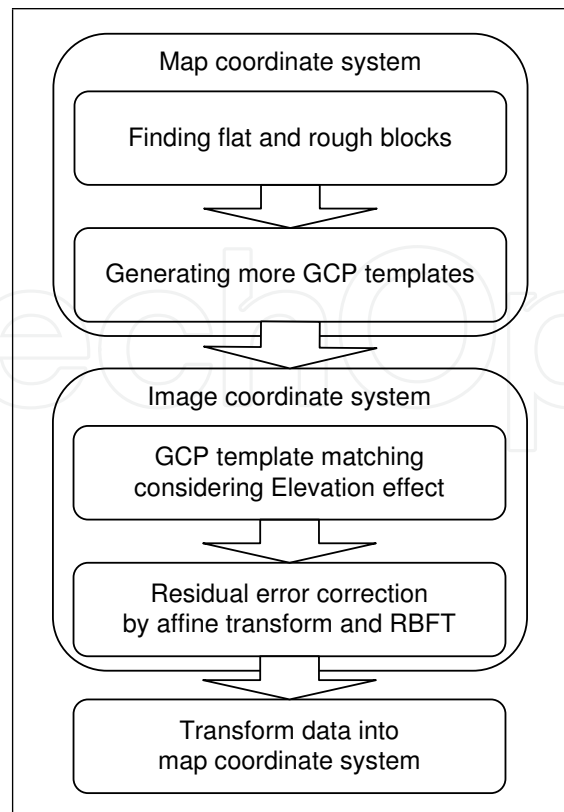


Fig. 7. Steps of the proposed method

Figure 8 is an example of the dividing a block into smaller flat and rough blocks. In figure 8a, an original block of 16x16 points is identified as a rough block, and it is divided into 4 smaller blocks of 8x8 points. The highest and lowest points in each smaller block are compared to find out one flat block (block 1) and three rough blocks (block 2, 3, 4). Each rough block in figure 8a continues to be divided into 4 smaller blocks of 4x4 points in figure 8b (from block 5 to block 16 in figure). The highest and lowest points in these 4x4 points blocks are compared to identify flat blocks (block 5, 7, 10, 14, 15, 16) and rough blocks (block 6, 8, 9, 11, 12, 13). In this study, a block is considered as a flat block if the difference in the elevation between the lowest and the highest point is smaller than 50m; otherwise, the block is considered as a rough block. The value 50m is selected as the threshold for a rough block because if the difference in elevation is greater than 50m, the elevation error on the high altitude regions at the left or right side of the image may be greater than 0.5 pixel, and when this value is rounded, it will become 1 pixel displacement.

4.3 Generating more GCP templates

In order to acquire residual errors precisely, the number of GCP templates using in GCP template matching is very important. The greater number of GCP templates is used in GCP template matching, the more residual errors are calculated precisely by GCP template matching. On some regions, because of the cloud effect or the feature of the terrain, GCP template cannot be found or the number of GCP templates is not enough for GCP template matching. Therefore, in addition to the templates in the GCP template database, a method which automatically generates GCP templates based on the feature of the coastline described by Nakano

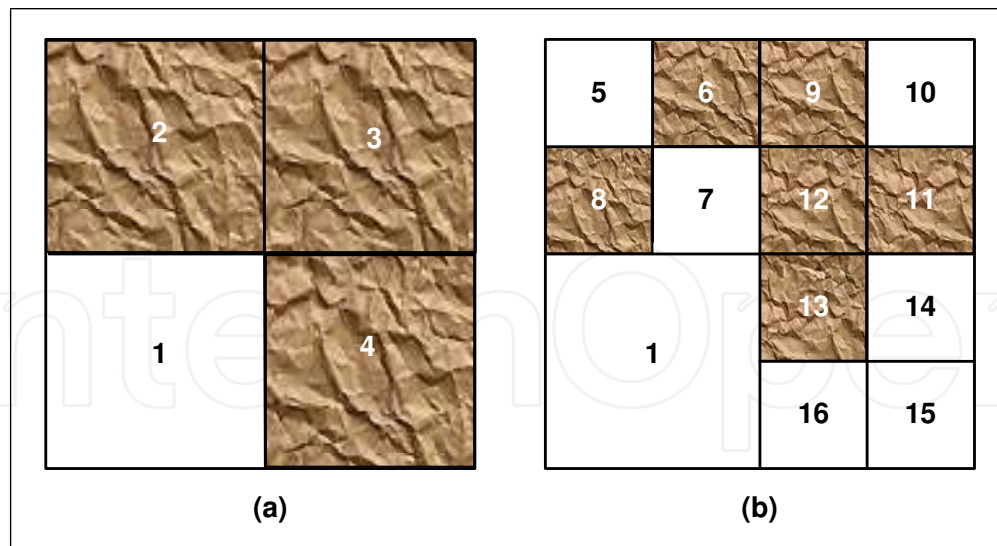


Fig. 8. Dividing data into flat and rough blocks

et al. (Nakano et al., 2004) is considered. According to this method, GCP templates are generated based on the feature of the coastline. The complexity in the shape of the coastline is taken into account to decide whether or not that region should become a GCP template.

GCP templates are generated automatically as following:

Firstly, the coastline image is created from the coastline database in the map coordinate system. A square of 33x33 points whose center is a point belonging to coastline is specified. In figure 9, a square of 33x33 points with center C_1 (belongs to the coastline) is created from the coastline image.

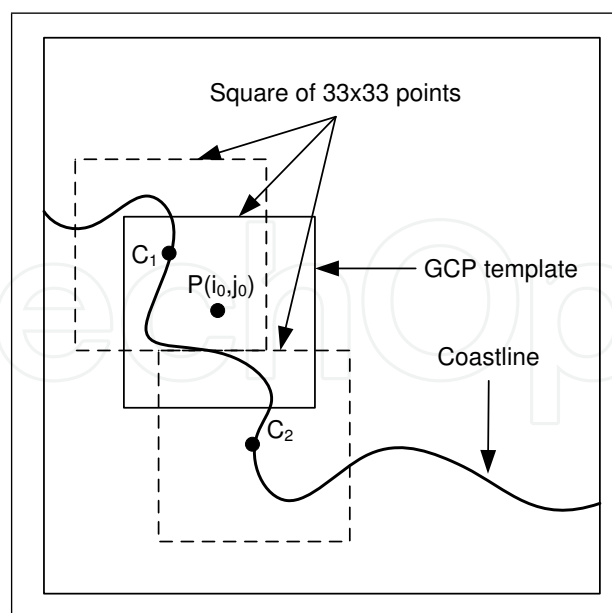


Fig. 9. Automatically generating GCP template

With every point p in this square, P is calculated as:

$$P(i, j) = \sum_{k=-r}^r \sum_{l=-r}^r c(i+k, j+l) \quad (7)$$

where (i, j) is the position of the point p , $r = 16$, and c is a function described by (8).

$$c(x, y) = \begin{cases} 1 & \text{if } (x, y) \text{ belongs to coastline} \\ 0 & \text{otherwise} \end{cases} \quad (8)$$

The values of P corresponding to the different positions of $p(i, j)$ are compared to find out the maximal value P_{max} . P_{max} is then compared with a threshold. If P_{max} is greater than that threshold, a square of 33x33 points, whose center is the point corresponding to P_{max} , is generated. And if this template is a flat region, it will be considered as a GCP template. In figure 9, $p(i_0, j_0)$ is supposed to correspond to P_{max} , and the square of 33x33 points whose center is $p(i_0, j_0)$ is generated. If P_{max} is greater than the threshold and this square locates on a flat region, it will be a GCP template.

Next, the square of 33x33 points, which locates next to the current square and whose center belongs to the coastline, is taken into account. In the figure 9, after finding GCP template in the square whose center is C_1 , the square whose center is C_2 will be considered.

This process is repeated until no more squares can be found. Figure 10 (Nakano et al., 2004) is an example of the GCP templates automatically generated by this method.

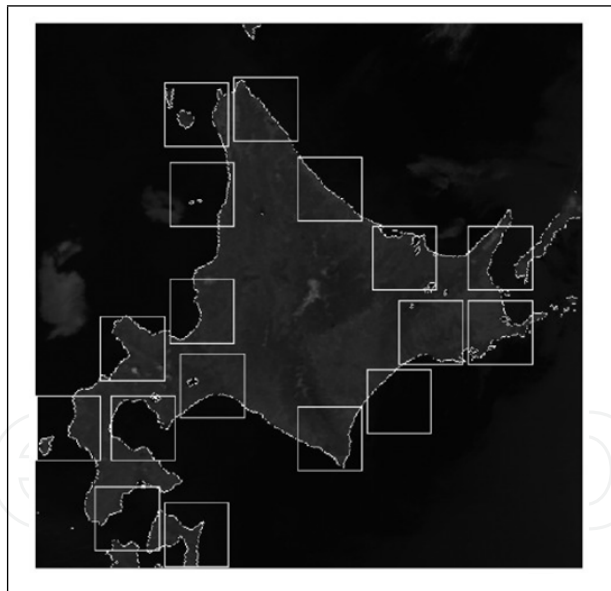


Fig. 10. A result of automatically generating GCP template

4.4 GCP template matching using reference data

Similar to the precise geometric correction method explained in the previous section, the result of GCP template matching is used to specify the residual errors. In the proposed method, both the GCP templates in the template database and the GCP templates generated automatically based on the features of the coastline are used for GCP template matching. GCP template matching is applied as it is described in the section 3.4.2.

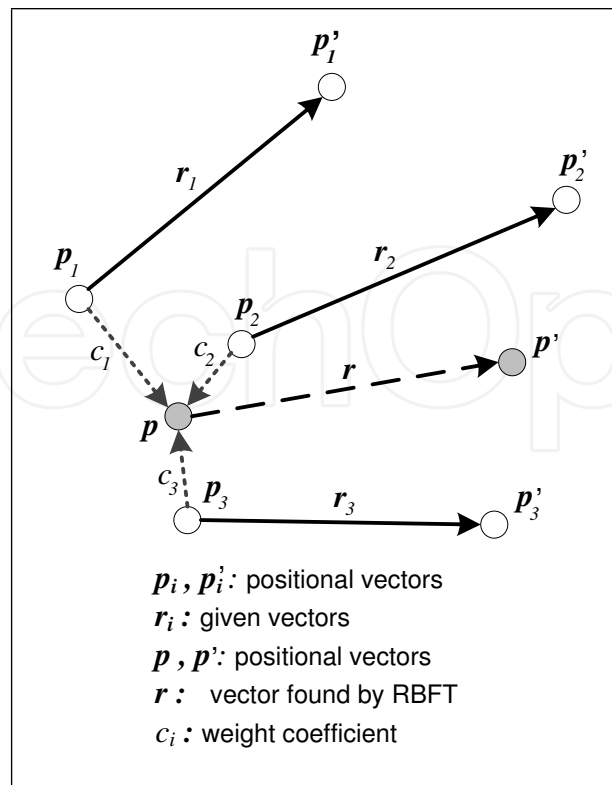


Fig. 11. Radial Basis Function Transform

4.5 Residual error correction considering affine transform and Radial Basis Function Transform

After GCP template matching, the residual errors of the GCP template's center points are found. In order to calculate the residual errors for the rest points in the NOAA image, some mathematical transformation is applied.

In a flat block, because the difference of the height between the highest and lowest points are quite small, the elevations of all points in this flat block are similar, and the variation of the elevation therefore can be considered as a linear variation. For this reason, in the proposed method, affine transform is applied to calculate the residual errors for only the points in the flat blocks.

In the rough blocks, the variation of elevation is more complicated than that in the flat blocks. Thus, rather than applying affine transform, another mathematical transformation should be used to calculate the residual errors in the rough blocks. Based on the fact that the elevation error of a point is affected more strongly by the elevation errors of its neighboring points than by the elevation errors of the further points, Radial Basis Function Transform (RBFT) (Pighin et al., 1998) is used to calculate the residual errors in the rough blocks.

Figure 11 shows an example of using RBFT. Supposed that N vectors r_i are already known, $i = \overline{1, N}$. p_i and p'_i is the positional vector of the start point and end point of vector r_i respectively. Based on the vectors r_i , p_i and p'_i , RBFT is applied to find the vector r whose start point is expressed by the positional vector p . In the formulas (9) and (10), $g(t)$ is the Radial Basis Function. Firstly, from the vectors r_i and the positional vectors p_i , the weight

coefficients c_j are found by (9):

$$\mathbf{r}_i = \sum_{j=1}^N c_j g(\|\mathbf{p}_i - \mathbf{p}_j\|) \quad (9)$$

Based on these weight coefficients, vector \mathbf{r} is calculated as (10):

$$\mathbf{r} = \sum_{i=1}^N c_i g(\|\mathbf{p} - \mathbf{p}_i\|) \quad (10)$$

By using RBFT, the smaller the distance from \mathbf{p} to \mathbf{p}_i is, the greater the vector \mathbf{r}_i affects to the vector \mathbf{r} .

In the proposed method, affine transform and RBFT are used to find the residual errors in the images as the following steps:

1. Use bilinear interpolation to find the positions in the image coordinate system for the points in the flat blocks. With the rough blocks, because the variation of elevation is complicated, the positions in the image coordinate system of all points in these blocks are found from the satellite's parameters and Earth's location.
2. Apply affine transform to calculate the residual errors for the points in the flat blocks.
3. With the rough blocks:
 - (a) Mark the center points of GCP templates as the calculated points. All the points in the rough blocks are marked as un-calculated points.
 - (b) With each un-calculated point, find its nearest GCP template.
 - (c) Find the un-calculated points whose distances from them to their nearest GCP templates are the shortest.
 - (d) With the points found in step (c), select the point whose elevation is the most similar to the elevation of its nearest GCP template.
 - (e) Apply RBFT to the residual error vectors of the calculated points to find the residual error vector for the point found in step (d). After the residual error is found, mark this point as a calculated point.
 - (f) Repeat from step (c) to step (e) until all the points in the rough blocks are calculated points.
4. All points in the image are moved to their corrected positions according to their residual error vectors.

By applying RBFT, the residual error vector of a point in a rough block is specified based on the residual error vectors of other points as well as the distances from the current point to those points. The shorter the distance between points is, the more strongly these points affect to each other. It reflects the real situation that the elevation error of a point is affected more strongly by its neighboring points' elevation errors than by the further points'.

4.6 Transforming data into map coordinate system

In the final step, data is transformed into the map coordinate system. By transforming data from the map coordinate system into the image coordinate system in the previous step, each point in the image coordinate system has its corresponding point in the map coordinate system. After moving all points in the image coordinate system to their correct positions according to their residual errors, the values of these points are assigned to their corresponding positions in map coordinate system.

As described in the previous step, because bilinear interpolation is applied only on the flat blocks, where the elevation errors of all points are fairly same, the error of bilinear interpolation is reduced. Furthermore, since satellite's parameters and Earth's location are used to transform data on the rough regions, the precision of transformation on the rough regions is high.

4.7 Result and Evaluation

The proposed method was applied to correct the errors for the NOAA images receiving in Tokyo (Japan), Bangkok (Thailand) and Ulaanbaatar (Mongolia). In order to evaluate the precision of the proposed method, the correction results of the precise geometric correction method (precise method) - described by Ono and Takagi (Ono & Takagi, 2001), and some different versions of the proposed method are compared.

In order to evaluate the correction results, some tests are performed. In each test, a number of NOAA images are corrected. With each NOAA image, 90% number of GCP templates are used for GCP template matching. After correction, the residual errors at the positions corresponding to the rest 10% number of GCP templates (which are used as the checking points) are acquired by using GCP template matching in the map coordinate system.

4.7.1 Selecting the radial basic function for RBFT

There are several types of radial basic function, which can be used for RBFT. In the proposed method, to express the fact that the elevation error of a point is affected by more strongly by the elevation errors of its neighboring points than by the elevation errors of the further points, the non-linear radial basis function whose shape is similar to the graph in the figure 12 is used. In this figure, the x axis is the distance between two points; the bigger the distance between two points is, the more weakly their errors affect to each other.

From the above shape, the most common radial basis function types including Gaussian function $g(t) = e^{-kt}$, Inverse-Multiquadric function $(1 + kt)^{-1/2}$ and Cauchy function $(1 + kt)^{-1}$ are considered. In order to select the best radial basic function for RBFT, these functions are applied to correct the distortions and the correction results are evaluated.

The value of k in each function is specified so that the residual error vectors of all the points in a NOAA image are used for RBFT. Because each NOAA image often includes 5000 lines, each line contains 2048 pixels, the maximum distance between two points in the image is around $\sqrt{(5000^2 + 2048^2)} \approx 5400$ pixels. This maximum distance should correspond to the minimum value of the radial basic function. Therefore, in the proposed method, the output of radial basic function should be nearly zero when the value of its variable is the maximum distance. In calculating, the minimum value of the radial basic function is selected to be equal to 10^{-6} .

Based on this idea, the best value of k for each radial basis function will be found by comparing the average error after correction of the tests on 100 NOAA images when the maximum distance is changed from 4000 pixels to 6000 pixels.

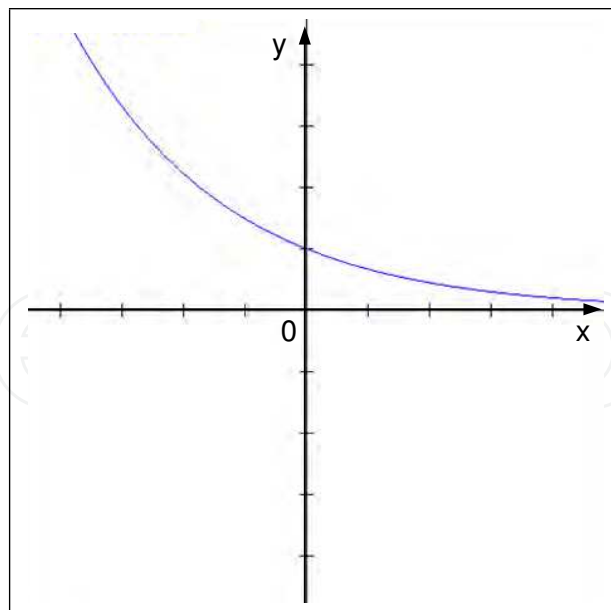


Fig. 12. The shape of the radial basic function

Table 1 is the result of this test. In this table, the average errors after correction in latitude and longitude directions are calculated for each type of radial basis function; G is Gaussian, I.M is Inverse Multiquadric and C is Cauchy; Lat is latitude and Lon is longitude.

Maximum Distance (pixels)	G		I.M.		C.	
	Lat	Lon	Lat	Lon	Lat	Lon
4000	0.25	0.28	0.31	0.35	0.33	0.40
4200	0.21	0.26	0.25	0.29	0.27	0.32
4400	0.16	0.20	0.23	0.26	0.23	0.27
4600	0.12	0.16	0.19	0.24	0.22	0.25
4800	0.15	0.17	0.22	0.25	0.23	0.26
5000	0.16	0.19	0.23	0.27	0.25	0.29
5200	0.17	0.21	0.23	0.29	0.27	0.31
5400	0.19	0.23	0.25	0.30	0.28	0.33
5600	0.21	0.25	0.25	0.32	0.30	0.34
5800	0.23	0.28	0.28	0.33	0.32	0.36
6000	0.25	0.30	0.29	0.35	0.34	0.39

Table 1. Average residual errors after correction with different maximum distances (unit: pixel)

This table shows that with each maximum distance, the Gaussian function is the best radial basic function because the average error of after correction when applying RBFT with this function is the smallest. This table also points out that the best maximum distance should be selected at around 4600 pixels, which corresponds to the value 0.003 of k in the Gaussian function.

4.7.2 Comparing affine transform and RBFT

The effectiveness of the affine transform and RBFT is compared by applying them to correct the same NOAA images and then finding the difference in the errors after correction.

In the first test, only the flat regions in 100 NOAA images are corrected by affine transform and then by RBFT. Table 2 is the results this test.

Image (Checking Points)	Value	Affine		RBFT	
		Latitude	Longitude	Latitude	Longitude
AH14060402222944 (45)	Average	0.12	0.15	0.11	0.13
	Maximum	1.00	1.00	1.00	1.00
	Minimum	0.00	0.00	0.00	0.00
AH16110602044118 (41)	Average	0.10	0.11	0.10	0.12
	Maximum	1.00	1.00	1.00	1.00
	Minimum	0.00	0.00	0.00	0.00
AH16110702183721 (46)	Average	0.12	0.14	0.11	0.14
	Maximum	1.00	2.00	1.00	1.00
	Minimum	0.00	0.00	0.00	0.00
100 NOAA images (44)	Average	0.11	0.12	0.10	0.12

Table 2. Residual errors after correction the flat regions by using affine transform and RBFT (unit: pixel)

Table 2 shows that, the average error after correction by affine transform and RBFT on the flat regions are not so different. Although the result of RBFT is a little better, affine transform will be selected for the proposed method because its computing cost is smaller than the one of RBFT.

In the second test, 100 NOAA images are corrected by the first method, which uses only affine transform, and the second method, which uses affine transform on the flat regions and RBFT on the rough regions. Table 3 is the results this test.

Table 3 shows that, compared with the correction results when applying only affine transform, the average error after correction is reduced 50% in latitude direction (0.22/0.44) and 49% in longitude direction (0.25/0.50) when applying affine transform on the flat regions and RBFT on the rough regions. It means that, compared with affine transform, RBFT reduces about 50% of the errors after correction on the rough regions.

4.7.3 Comparing the correction result of the precise method and the proposed method

In this test, the correction results of the proposed method are compared with those of the precise method. 100 NOAA images are corrected by the proposed method and the precise method. Table 4 shows the result of acquiring residual errors after correction. The average, maximum and minimum values of the residual errors in latitude and longitude direction are recorded. It is seen that both methods give highly accurate correction results, but the residual errors after correction of the proposed method are much smaller than the one of the precise method. The smaller residual errors after correction proved that the proposed method is more accurate than the precise method.

Figure 13 shows the correction results (in the map coordinate system) of the precise method (left pictures) and the proposed method (right pictures) on two regions of China where the

Image (Checking Points)	Value	Affine only		Affine and RBFT	
		Latitude	Longitude	Latitude	Longitude
AH14060402222944 (45)	Average	0.53	0.64	0.24	0.27
	Maximum	1.00	1.00	1.00	1.00
	Minimum	0.00	0.00	0.00	0.00
AH16110602044118 (41)	Average	0.37	0.62	0.22	0.27
	Maximum	1.00	2.00	1.00	1.00
	Minimum	0.00	0.00	0.00	0.00
AH16110702183721 (46)	Average	0.41	0.45	0.21	0.23
	Maximum	1.00	2.00	1.00	1.00
	Minimum	0.00	0.00	0.00	0.00
100 NOAA images (44)	Average	0.44	0.51	0.22	0.25

Table 3. Residual errors after correction by using affine transform and by using both affine transform and RBFT (unit: pixel)

elevation are 4392m and 4831m. In each picture, the black object is generated in the map coordinate system from the coastline database; the white curve is the result of geometric correction, it is the border of the black object. The black objects in all pictures should fit their white borders. The better geometric correction is, the better the black objects fit their white borders.

From the pictures in the figure 13, it is easy to see that, at both elevations (4392m and 4831m), the black objects fit their white borders in the right pictures (which are the result of the proposed method) better than those in the left pictures (which are the result of the precise method).

Figures 14 and 15 show the residual error vectors after correction (in the map coordinate system) of the precise method and the proposed method for the NOAA images AH16110602044118 and AH16110702183721, respectively. The vectors in these pictures are the residual error vectors after correction. It is clear that the residual error vectors after correction are improved by the proposed method. On some regions where the residual error vectors are big in the result of the precise method, the residual error vectors in the result of the proposed method are smaller.

4.7.4 Comparing the correction result of the proposed method and other methods

In this test, the correction results of the proposed method (method P) are compared with those of other two methods. Method S is systematic method, which just transforms data from the image coordinate system into map coordinate system by using bilinear interpolation (Ono & Takagi, 2001). Method C is conventional method, which correct data using GCP template matching but does not consider the elevation effect (Ono & Takagi, 2001). 02 NOAA images are corrected by these methods. Table 5 shows the result of acquiring residual errors after correction. The average, maximum and minimum values of the residual errors in latitude (Lat) and longitude (Lon) direction are recorded. It is seen that the residual errors after correction of the proposed method are much smaller than other two methods.

Image (Checking points)	Value	Precise Method		Proposed Method	
		Latitude	Longitude	Latitude	Longitude
AH14060402222944 (Precise:37/Proposed:45)	Average	0.53	0.64	0.17	0.20
	Maximum	1.00	1.00	1.00	1.00
	Minimum	0.00	0.00	0.00	0.00
AH16110602044118 (Precise:36/Proposed:41)	Average	0.37	0.62	0.12	0.17
	Maximum	1.00	2.00	1.00	1.00
	Minimum	0.00	0.00	0.00	0.00
AH16110702183721 (Precise:38/Proposed:46)	Average	0.41	0.45	0.11	0.14
	Maximum	1.00	2.00	1.00	1.00
	Minimum	0.00	0.00	0.00	0.00
100 NOAA images (Precise:38/Proposed:44)	Average	0.44	0.51	0.12	0.16

Table 4. Residual errors after correction by the precise method and proposed method (unit: pixel)

Image	Value	S		C		P	
		Lat	Lon	Lat	Lon	Lat	Lon
AH12102499232725	Average	3.00	3.40	0.50	0.90	0.18	0.22
	Maximum	5.00	12.00	2.00	3.00	1.00	1.00
	Minimum	1.00	1.00	0.00	0.00	0.00	0.00
AH14092199212611	Average	1.27	3.00	0.60	0.90	0.16	0.19
	Maximum	2.00	6.00	2.00	4.00	1.00	1.00
	Minimum	1.00	1.00	0.00	0.00	0.00	0.00

Table 5. Residual errors after correction by the proposed method and other methods (unit: pixel)

4.7.5 Evaluating the contribution of the steps in the proposed method

In this test, 100 NOAA images are corrected by three methods:

- M1: this is the proposed method without generating more GCP templates
- M2: this is the proposed method

Table 6 shows the average residual errors after correction by M1 and M2. When comparing the results of M1 and the precise method (in table 4), it can be seen that M1 reduces the errors considerably by dividing data into flat and rough blocks as well as applying both affine transform and RBFT to correct residual errors. After generating more GCP templates based on the feature of the coastline, the errors after correction are considerably reduced with M2.

Image	Value	M1		M2	
		Lat	Lon	Lat	Lon
100 NOAA images	Average	0.22	0.25	0.12	0.16

Table 6. Average residual errors after correction by M1 and M2 (unit: pixel)

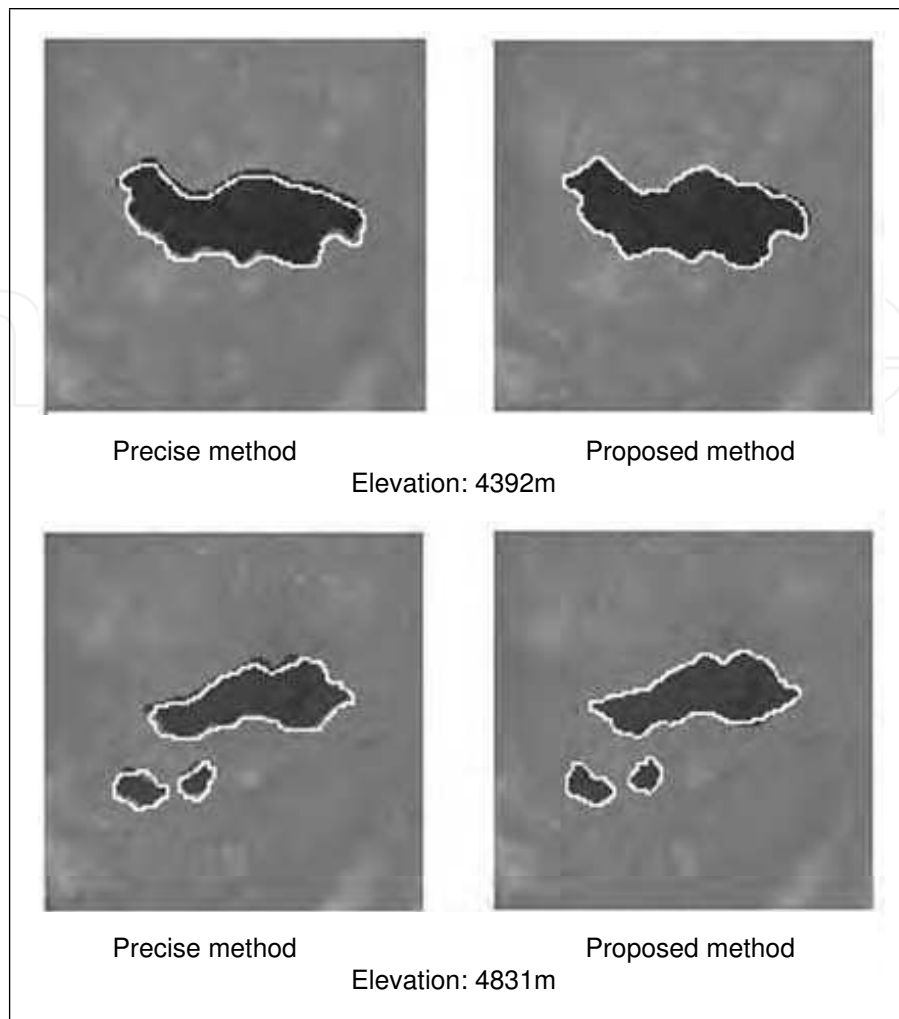


Fig. 13. Correction result of precise method and proposed method

4.7.6 Evaluating the processing time

Table 7 shows the processing time of the precise method and the proposed method. 100 NOAA images are processed by both methods on the computer Sun Ultra 45 Workstation with 1.6GHz Sun UltraSPARC IIIi processor and 1GB RAM. In these tests, all 5 channels of each image are corrected and the mapping unit is 0.01 degree. The maximum, minimum and average processing time of all channels are calculated. From the table 7, it is possible to say that, though the proposed method takes longer processing time, the difference between two methods is acceptable.

4.8 Discussion

This section proposed a novel geometric correction method for NOAA AVHRR data. The correction results have shown that the precision of the proposed method is high. Compared with the precise geometric correction method, which is described by Ono and Takagi (Ono & Takagi, 2001), the proposed method has some advantages:

- Data is divided into flat and rough blocks by identifying the variation of elevation. This dividing allows the errors in the different regions to be corrected in different ways.

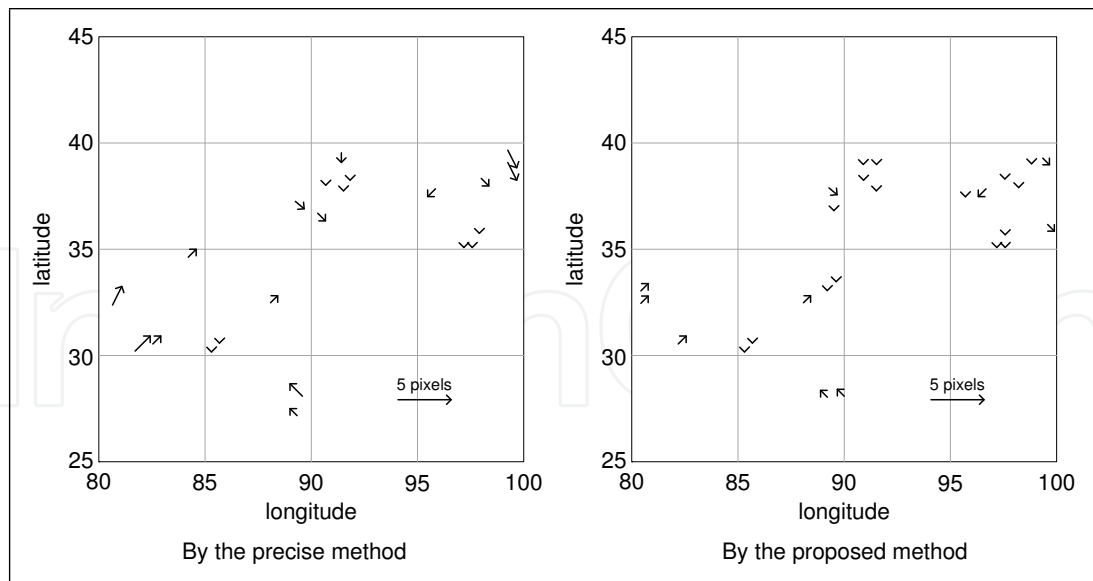


Fig. 14. Residual error vectors after correction the image AH16110602044118 by the precise method and the proposed method

Time	Precise Method	Proposed Method
Maximum	377.16 sec	390.17 sec
Minimum	359.49 sec	375.42 sec
Average	368.27 sec	381.48 sec

Table 7. Average processing time of 100 images

- Missing lines and noise pixels are corrected before applying GCP template matching. This improves the result of GCP template matching.
- The number of GCP templates is increased by automatically generating more GCP templates based on the feature of the coastline. With more GCP templates, more residual errors are acquired precisely by GCP template matching.
- Residual errors on the flat regions are corrected by affine transform; residual errors on the rough regions are corrected by RBFT with Gaussian radial basis function. With RBFT, the residual errors on the rough regions are corrected more accurately.
- Bilinear interpolation is applied only on the flat regions. This reduces the errors of bilinear interpolation on the rough regions, where the variation of elevation is big.

Besides the advantages, the proposed method also has some problems:

- If the interest region is a flat region, the precise method and the proposed method may produce the same correction results; however, the proposed method will take longer processing time because it needs time to identify the flat and rough regions.
- There is no relationship in the residual error correction results between flat and rough regions. The residual error correction results on the flat regions are not considered when correcting residual errors on the rough regions. Therefore, there is a case that two neighboring points with the same elevation error, one belongs to a flat region, another

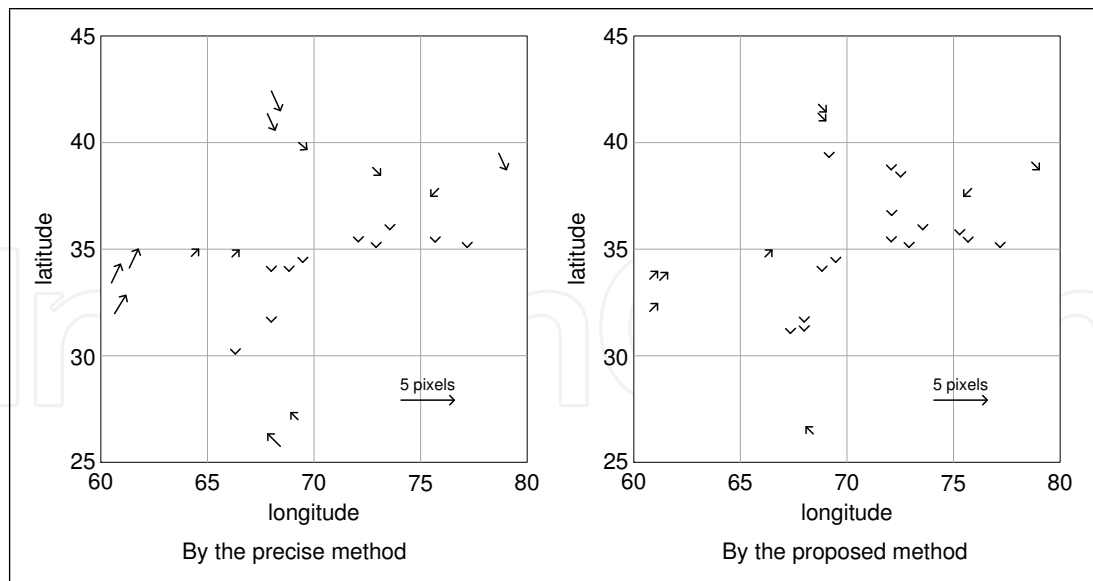


Fig. 15. Residual error vectors after correction the image AH16110702183721 by the precise method and the proposed method

belongs to a rough region, will have quite different residual errors because they are corrected by different methods.

4.9 Conclusion of future works

This book chapter proposed a novel highly accurate geometric correction method considering the variation of elevation effect.

With the proposed method, the data in the map coordinate system is divided into flat and rough blocks in order to identify the variation of elevation. More GCPs are generated based on the features of the coastline. Residual errors are specified in the image coordinate system by GCP template matching and they are corrected based on the variation of elevation. Affine and RBFT is used to correct the residual errors on flat rough blocks, respectively. For this reason, residual errors are corrected more precisely. When transforming data into the map coordinate system, bilinear interpolation is applied only on the flat blocks; satellite's parameters and earth's location are used to transform data on rough blocks. Therefore, the precision of this transformation process is higher.

With higher precision and the processing time is not too different compared to the precise geometric correction method, it is possible to say that the proposed method has higher efficiency than the precise geometric correction method. It can be integrated into some NOAA AVHRR processing applications such as PaNDA (Yasuoka and Takeuchi Laboratory, 2006) to improve the processing results. NOAA images corrected by this algorithm can also be easier to combine with other high-resolution types satellite image to complete other processing operations.

The correction results of proposed method show that the errors still exist after correction. In order to improve the correction result, some future works should be taken into account. Firstly, the number of GCPs and their precision can be increased by combination of the proposed method in this book chapter with the characteristics of the terrain, not only the feature of the coastline but also the information from the better database or from the higher resolution satellite images. Next, some new mathematical transformations should be considered

to select the appropriate transformations between the image coordinate system and the map coordinate system. Finally, other geometric correction methods, which have been applied for the high resolution satellite images can be a good references for NOAA images.

5. References

- Bannari, A.; Morin, D.; Benie, G. B.; Bonn, F. J. (1995). A theoretical review of different mathematical models of geometric corrections applied to remote sensing images, *Remote sensing reviews*, pp.27-47, Vol.13.
- Brush, R. J. H. (1985). A method for real-time navigation of AVHRR imagery, *IEEE Transactions on Geoscience and Remote Sensing*, pp.876-887, Vol.23.
- Crawford, P. S.; Brooks, A. R.; Brush, R. J. H. (1996). Fast navigation of AVHRR images using complex orbital models, *International Journal of Remote Sensing*, pp.197-212, Vol. 17.
- Gibson, P. G. & Power, C. H. (2000). *Introductory Remote Sensing, Digital image processing and applications*, Routledge, England.
- Landgrebe, D. A. (1980). The development of a spectral spatial classifier for Earth observation data, *Journal of Pattern recognition*, pp.165-175, Vol.12, Issue 3.
- Mather, P. M. (2004). *Computer Processing of Remotely-Sensed Images*, Third Ed., John Wiley & Sons, ISBN, England.
- Moreno, J. F. & Melia, J. (1993). A method for accurate geometric correction for NOAA AVHRR HRPT data, *IEEE Transactions on Geoscience and Remote Sensing*, pp.204-226, Vol.31, No. 3.
- Murai, S. (1980). Geometric and Geographic Correction for Remote Sensing Data, *Proceedings of Asian Conference on Remote Sensing*, <http://www.gisdevelopment.net/aars/acrs/1980/techsa/techs002pf.htm>.
- Nakano, M.; Kalpoma, K.; Kudoh, J. (2004). Automatic GCP creation for NOAA AVHRR geometric correction, *Proceedings of IEEE International Geoscience and Remote Sensing Symposium*, pp.3733-3735.
- NASA, (2002). NOAA-17 (M) Environmental Satellite Successfully Launched, <http://earthobservatory.nasa.gov/Newsroom/view.php?old=200206249448>.
- NOAA, (1998). NOAA Polar Orbiter Data User's Guide, <http://www2.ncdc.noaa.gov/docs/podug/index.htm>.
- NOAA, (2000). NOAA KLM User's guide, <http://www.ncdc.noaa.gov/oa/pod-guide/ncdc/docs/klm/index.htm>.
- NOAA Satellites and Information Service, (2008). NOAA's Geostationary and Polar-Orbiting Weather Satellites, <http://noaasis.noaa.gov/NOAASIS/ml/genlsatl.html>.
- NOAA Satellites and Information Service, (2008). Advanced Very High Resolution Radiometer - AVHRR, <http://noaasis.noaa.gov/NOAASIS/ml/avhrr.html>.
- Ono, T. & Takagi, M. (2001). Precise Geometric Correction of NOAA Satellite imagery Considering Elevation effects, *Proceedings of International Symposium on Remote Sensing*, pp.378-388, Vol.31, No.3.
- Purevdorj, T., Yokoyama, R. (2000). Geometric Registration Method For 10-Day Composite AVHRR Data For Asian Region, *Proceedings of Asian conference on remote sensing*, <http://www.gisdevelopment.net/aars/acrs/2000/ts9/imgp0015.asp>.
- Pighin, F.; Hecker, J.; Lichinski, D. (1998). Synthesizing realistic facial expressions from photographs, *Proceedings of SIGGRAPH98*, pp.75-84.

- Saitoh, K.; Hashimoto, T.; Kajiwara, K.; Tateishi, R. (1995). Geometric Correction of NOAA AVHRR GAC Data, *Proceedings of Asian conference on remote sensing*, <http://www.gisdevelopment.net/aars/acrs/1995/ts5/ts5006.asp>.
- Takagi, M. (2003). Precise geometric correction for NOAA and GMS images considering elevation effects using GCP template matching and affine transform, *Proceedings of SPIE Conference on Remote Sensing, Image and Signal Processing for Remote Sensing IX*, pp.132-141, Vol. 5238, Barcelona, Spain.
- Tozawa, Y. (1983). Fast Geometric correction of NOAA AVHRR, *Proceedings of Symposium on machine processing of remotely-sensed data*, pp.46-53.
- Yasukawa, M.; Takagi, M.; Kitsuregawa, M. (2004). High-speed and precise geometric correction for GMS S-VISSR data, *Proceedings of IEEE International Geoscience and Remote Sensing Symposium*, pp.3970-3973. Vol. 6.
- Yasuoka and Takeuchi Laboratory (2006). WebPaNDA - NOAA AVHRR data processing, <http://webpanda.iis.u-tokyo.ac.jp/>.

IntechOpen

IntechOpen

IntechOpen



Geoscience and Remote Sensing New Achievements

Edited by Pasquale Imperatore and Daniele Riccio

ISBN 978-953-7619-97-8

Hard cover, 508 pages

Publisher InTech

Published online 01, February, 2010

Published in print edition February, 2010

Our planet is nowadays continuously monitored by powerful remote sensors operating in wide portions of the electromagnetic spectrum. Our capability of acquiring detailed information on the environment has been revolutionized by revealing its inner structure, morphology and dynamical changes. The way we now observe and study the evolution of the Earth's status has even radically influenced our perception and conception of the world we live in. The aim of this book is to bring together contributions from experts to present new research results and prospects of the future developments in the area of geosciences and remote sensing; emerging research directions are discussed. The volume consists of twenty-six chapters, encompassing both theoretical aspects and application-oriented studies. An unfolding perspective on various current trends in this extremely rich area is offered. The book chapters can be categorized along different perspectives, among others, use of active or passive sensors, employed technologies and configurations, considered scenario on the Earth, scientific research area involved in the studies.

How to reference

In order to correctly reference this scholarly work, feel free to copy and paste the following:

An Ngoc Van, Mitsuru Nakazawa and Yoshimitsu Aoki (2010). Highly Accurate Geometric Correction for NOAA AVHRR Data, *Geoscience and Remote Sensing New Achievements*, Pasquale Imperatore and Daniele Riccio (Ed.), ISBN: 978-953-7619-97-8, InTech, Available from: <http://www.intechopen.com/books/geoscience-and-remote-sensing-new-achievements/highly-accurate-geometric-correction-for-noaa-avhrr-data>

INTECH
open science | open minds

InTech Europe

University Campus STeP Ri
Slavka Krautzeka 83/A
51000 Rijeka, Croatia
Phone: +385 (51) 770 447
Fax: +385 (51) 686 166
www.intechopen.com

InTech China

Unit 405, Office Block, Hotel Equatorial Shanghai
No.65, Yan An Road (West), Shanghai, 200040, China
中国上海市延安西路65号上海国际贵都大饭店办公楼405单元
Phone: +86-21-62489820
Fax: +86-21-62489821

© 2010 The Author(s). Licensee IntechOpen. This chapter is distributed under the terms of the [Creative Commons Attribution-NonCommercial-ShareAlike-3.0 License](#), which permits use, distribution and reproduction for non-commercial purposes, provided the original is properly cited and derivative works building on this content are distributed under the same license.

IntechOpen

IntechOpen